Mechatronics 43 (2017) 1–5

Contents lists available at ScienceDirect

Mechatronics

journal homepage: www.elsevier.com/locate/mechatronics

Control of high-precision direct-drive mechatronic servos: Tracking control with adaptive friction estimation and compensation☆

Sergey Edward Lyshevski

Department of Electrical and Microelectronic Engineering, Rochester Institute of Technology, Rochester, NY 14623-5603, USA

ARTICLE INFO

Article history:
Received 20 September 2016
Revised 6 February 2017
Accepted 13 February 2017

Keywords:
Actuators
Control
Friction
Mechatronics
Servo

ABSTRACT

This paper examines nonlinear mechatronic systems with direct-drive limited-angle axial-topology actuators. The considered direct-drive servos are used in hard disk drives, manipulators, pointing systems, robots, rotating platforms, aerial vehicles, etc. High accuracy, precision and fast repositioning should be ensured despite friction and adverse phenomena which degrade overall performance and capabilities. Tracking control laws which compensate friction using the estimated parameters are designed. The adverse friction is compensated by a nonlinear feedback. Adaptive reconfiguration is ensured by estimating the unknown parameters in near real-time. Design and technological challenges are overcome by a consistent paradigm and hardware-centric concurrent design. The concept and solutions are experimentally verified.

1. Introduction

Direct-drive servos with samarium-cobalt (SmCo) and neodymium-iron-boron (NeFeB) magnets guarantee high torque density, efficiency, robustness, simplicity, reliability and other enabling capabilities [1–4]. These actuators are widely used in aerospace, automotive, robotic and other applications. Different design concepts for hard disk drives and pointing servos are reported in [1–10]. The servos must guarantee accuracy, precision, fast repositioning, etc. The direct-drive servos with axial-topology limited-angle actuators ensure simple compliant kinematics, minimal losses, high acceleration, minimal friction and other advantages compared to other solutions, including servos with precision planetary gearheads. The arcminute (2.9×10^{-4} rad) accuracy may not be ensured by advanced-technology servos with high-precision gearheads. To approach the arcminute-range accuracy, one must: (1) Implement direct-drive kinematics; (2) Use high-precision sensors and advanced microelectronics; (3) Design and implement control algorithms to reduce and compensate adverse phenomena such as friction, perturbations, etc. Advanced-technology rotary encoders, resolvers, synchros and variable differentiable transformers may ensure the arcminute errors in measuring of angular displacement. Friction, lubrication, asymmetry, eccentricity, kinematic imperfections and other phenomena cause significant challenges [3,11–14].

Nonlinear control concepts were applied to design high-performance mechatronic systems. Control laws were derived applying dynamic programming, maximum principle and nonlinear optimization methods. Significant challenges arise when physical systems are examined. Closed-loop systems with microelectronics, power electronics, actuators, sensors and microcontrollers must be implemented, and, hardware limits should be overcome. Application of theoretical concepts, applied to physical servos, may not guarantee the expected performance and implementation abilities. A concurrent technology-centric design is developed and experimentally substantiated. The friction compensating feedback is derived by examining nonlinear friction and estimating time-varying parameters. The experiments demonstrate that adequate controllers with nonlinear feedback guarantee accurate repositioning, precision and high bandwidth. The high-accuracy sensor measures the displacement and estimates the angular velocity. We propose new solutions to a spectrum of pertinent engineering and technological problems in design and implementation of high-precision servos.

2. Direct-drive servo kinematics and analyses

2.1. Axial topology actuators in mechatronic systems

High torque density permanent-magnet actuators directly actuate the rotating kinematics as shown in Fig. 1a. The direct-drive servo is controlled by the PWM *driver* which changes the applied voltage, see Fig. 1b. The rotating resolver measures the angular displacement.

☆ This paper was recommended for publication by Associate Editor Kenn Oldham.

E-mail address: Sergey.Lyshevski@mail.rit.edu

http://dx.doi.org/10.1016/j.mechatronics.2017.02.005
0957-4158/

Nomenclature

a	is the magnetization and dimension-dependent constant of the segmented magnets
B_{mi}, b_i and c_i	are the time-varying friction parameters
B and $B_{\max}$	are the magnetic flux density and magnet flux density as viewed from a planar coil
e and Δe	are the tracking error and steady-state error
i_a	is the current in the coils
J	is the moment of inertia
F_e	is the electromagnetic force
k_p, k_i and k_d	are the proportional, integral and derivative feedback gains
k_s	is the constant
l_{eq}	is the coil active length
L_a	is the winding self-inductance
N	is the number of turns
r_a	and Δr_a are the winding resistance and variation of the resistance
$R_\perp$	is the perpendicular radius
T_e	is the electromagnetic torque
T_{friction} and T_d	are the friction and disturbance (perturbation) torques
T_s	is the restoring torsional torque of spring or minimagnets
u_a	is the applied voltage
ψ	is the flux linkage
ω_r and θ_r	are the angular velocity and displacement
θ_L and θ_R	are the relative angular displacements of the left and right coil filaments
$\theta_{L0} = \theta_{R0} = \theta_{r\max}$	is the maximum displacement angle

Using the Kirchhoff and Newton's law, the *circuitry-electromagnetic* and *torsional-mechanical* equations of motion are

$$u_a = r_a i_a + \frac{d\psi}{dt},\quad \frac{d\omega_r}{dt} = \frac{1}{J}(T_e - T_{\text{friction}} - T_d - T_s),\quad \frac{d\theta_r}{dt} = \omega_r. \quad (1)$$

The magnetic coupling between the winding (*current loop*) and segmented NeFeB magnets results in the electromagnetic torque. The electromagnetic force is $T_e = R_\perp F_e = -R_\perp i_a B \times \int dl$. Consider a segmented array of two NeFeB magnets. The planar winding is in an uniform magnetic field, $B(\theta_r) = B_{\max}\tanh(a\theta_r)$. Hence, $T_e = R_\perp l_{eq} N B_{\max}(\tanh a\theta_L + \tanh a\theta_R) i_a$, $\theta_L(t) = \theta_{L0} - \theta_r(t)$, $\theta_R(t) = \theta_{R0} + \theta_r(t)$, $\theta_{L0} = \theta_{R0} = \theta_{r\max}$, $-\theta_{r\max} \le \theta_r \le \theta_{r\max}$.

The motional *emf* is $\mathcal{E} = -N\frac{d}{dt}\int_{r_{\text{in}}}^{r_{\text{out}}}\int_{\theta_R}^{\theta_L} B_{\max}\tanh(a\theta_r) r dr d\theta_r = -\frac{r_{\text{out}}^2 - r_{\text{in}}^2}{2} N B_{\max}(\tanh a\theta_L - \tanh a\theta_R)\omega_r$.

A set of nonlinear differential equations is

$$\begin{aligned}
\frac{di_a}{dt} &= \frac{1}{L_a}\left[-r_a i_a - \frac{r_{\text{out}}^2 - r_{\text{in}}^2}{2} N B_{\max}[\tanh a(\theta_{L0} - \theta_r) - \tanh a(\theta_{R0} + \theta_r)]\omega_r + u_a\right],\\
\frac{d\omega_r}{dt} &= \frac{1}{J}[R_\perp N l_{eq} B_{\max}(\tanh a\theta_L + \tanh a\theta_R) i_a - T_{\text{friction}} - T_d - T_s],\ T_s = k_s\theta_r,\\
\frac{d\theta_r}{dt} &= \omega_r,\ -\theta_{r\max} \le \theta_r \le \theta_{r\max}.
\end{aligned} \quad (2)$$

In high-performance actuators $a \gg 1$, and $\tanh a\theta_R = \tanh a\theta_L \approx 1$, $\theta_i \ne 0$. Hence, $T_e = T_{eR} + T_{eL} = 2R_\perp N l_{eq} B_{\max} i_a$ and $\mathcal{E} = -(r_{\text{out}}^2 - r_{\text{in}}^2) N B_{\max}\omega_r$. For $a >> 1$, one finds

$$\begin{aligned}
\frac{di_a}{dt} &= \frac{1}{L_a}\left[-r_a i_a - (r_{\text{out}}^2 - r_{\text{in}}^2) N B_{\max}\omega_r + u_a\right],\\
\frac{d\omega_r}{dt} &= \frac{1}{J}[2R_\perp N l_{eq} B_{\max} i_a - T_{\text{friction}} - T_d - k_s\theta_r],\\
\frac{d\theta_r}{dt} &= \omega_r,\quad -\theta_{r\max} \le \theta_r \le \theta_{r\max}.
\end{aligned} \quad (3)$$

2.2. Mathematical models of friction with experimental substantiation

In simplified analysis, the friction torque is approximated as $T_{\text{friction}} = B_m\omega_r$. To design high-performance servos, the friction torque T_{friction} must be accurately measured and characterized. The static and dynamic frictions are studied in [3,11–14]. The steady-state and differential equations are proposed using the fluid lubrication hydrodynamics, dynamic viscosity, solid and fluid frictions on geometrical surfaces, surfaces interaction, and other phenomena. For the viscous and Coulomb frictions, the following expressions are derived [3,11–14]

$$T_{\text{friction}} = B_m\omega_r + b\,\mathrm{sgn}(\omega_r)\left(1 - e^{-c|\omega_r|}\right),\ T_{\text{friction}} = B_m\omega_r + b\,\mathrm{sgn}(\omega_r)\left(1 - e^{-c\omega_r^2}\right),\ b > 0 \text{ and } c > 0. \quad (4)$$

Inherent time-varying asymmetry, lubrication, surface nonuniformity, wearing, varying loads, temperature, surface roughness and other phenomena significantly affect friction. The general expression derived and experimentally substantiated is [3]

$$\begin{aligned}
T_{\text{friction}} &= \sum_i B_{mi}\,\mathrm{sgn}(\omega_r)|\omega_r|^{\frac{i}{1+2\mu_1}} + \sum_j B_{mj}\omega_r^{j+2\mu_2}\\
&\quad + \mathrm{sgn}(\omega_r)\left[\sum_i b_i\left(1 - e^{-c_i|\omega_r|^{i/(1+2\gamma_1)}}\right) + \sum_j b_j\left(1 - e^{-c_j|\omega_r|^{j+2\gamma_2}}\right)\right],\\
\mu_i &= 0, 1, \ldots \text{ and } \gamma_i = 0, 1, \ldots
\end{aligned} \quad (5)$$

The experimentally measured T_{friction} for the angular velocity envelope $\omega_r \in [-25\ 25]$ rad/sec is reported in Fig. 2. Using (5), for

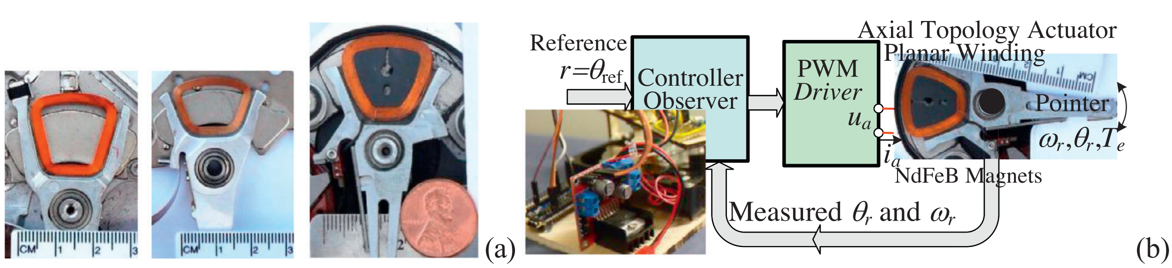

Fig. 1. (a) Axial topology actuators: Rotating direct-drive kinematics with deposited winding above the nickel-plated $Nd_2Fe_{14}B$ magnets; (b) Closed-loop servo: Kinematics – actuator – sensors – PWM *driver* – controller.